Visualization of Detonation Propagation in a Round Tube Equipped with Orifice Plates

Georgina Rainsford and Gabriel Ciccarelli
Queen's University
Kingston, Ontario, Canada

1 Introduction

The propagation of a detonation wave past a series of obstacles has been studied for many years. The first comprehensive study performed by Peraldi et al. [1] in different diameter metal round tubes equipped with orifice plates. Diagnostics was restricted to flame time-of-arrival measurements that were used to obtain the average steady-state combustion front velocity. They showed that there is a sharp transition from choked flame to detonation propagation that correlates with cell size. Lieberman and Lee [2] used self-luminous streak photography through a narrow slit at the centerline of a plastic tube filled with orifice plates to track detonation and choked flame propagation. Recently, Cross and Ciccarelli [3] recorded the detonation wave front triple-point tracks using soot foils placed on the tube wall between orifice plates. The study provided evidence that for fuel-air mixtures at conditions where the orifice diameter is less than 13 times the cell size ($d<13\lambda$) the detonation propagation mechanism involves successive cycles of detonation wave failure and re-initiation. Based on the soot foil records, the authors proposed that detonation re-initiation occurred at the tube wall following the reflection of the diffracting shock wave emerging from the preceding orifice plate. At the propagation limits, re-initiation typically occurred at a single hot spot. There was no evidence of single head-spin, normally associated with propagation at the limit in a smooth walled tube, as reported by Starr et al. [4]. The propagation mechanism for a detonation wave in a rectangular-channel equipped with obstacles has been investigated [5, 6] using high-speed Schlieren photography. The objective of this study is to use self-luminous high-speed photography to investigate the detonation propagation in a round tube equipped with repeating orifice plates.

2 Experiment

Experiments were conducted in a 3.16 m long aluminum combustion channel with a 7.62 cm square cross-section connected to an Acrylic 1.55 m long, 7.62 cm inner-diameter cylindrical combustion channel. 'Fence-type' obstacles of 7.62 cm height, 1.91 cm width and 1.27 cm length were spaced every 6.35 cm along the top and bottom sides of the square channel, providing a 50% obstacle blockage ratio. The same blockage ratio and spacing was maintained in the cylindrical section using 5.33 cm diameter orifice plates and 1.27 cm long, 7.62 cm inner-diameter cylindrical spacers, respectively. The spacers also prevent any possible leakage of gas around the outside of the orifice plates. Self-luminous high-speed video (up to 300,000 frames per second) was captured perpendicular to the combustion channel through the optically clear Acrylic tube using a Photron SA-Z camera. A synchronized Photron SA-5 camera was used to capture video at a head-on view through a 7.62 cm x 7.62 cm glass window at the end of the tube (for these tests Acrylic orifice plates were used). PCB pressure transducers installed in the last square channel were used to determine the average wave velocity entering the cylindrical section. Premixed stoichiometric hydrogen-oxygen mixtures at initial pressures of 7.5 - 60 kPa were ignited via an automotive capacitive discharge system at one end of the channel. Mixtures at initial pressures less than 7 kPa were ignited using a standard automotive glow plug. For some tests, an aluminum soot foil was installed inside the cylindrical combustion chamber, between obstacles 9 and 10 as shown in Figure 1.

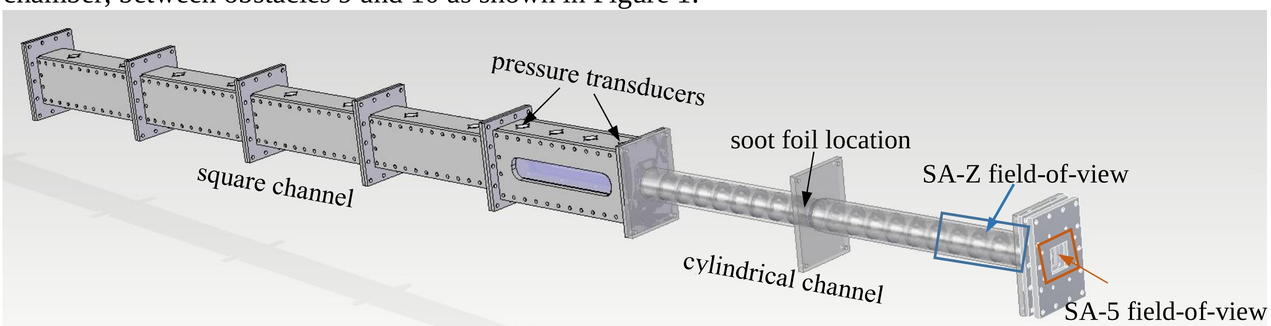

Figure 1: Model of the experimental apparatus

3 Results and Discussion

The average wave front velocity measured in the last square channel and in the cylindrical channel over the camera field-of-view (across five orifice plates as shown in Figure 1) as a function of the initial pressure are plotted in Figure 2. Also plotted for reference, are the theoretical CJ detonation velocity and the speed of sound in the combustion product calculated for an adiabatic isobaric process. The detonation limit, defined by an average velocity that exceeds the isobaric speed of sound, is 10 kPa in the square channel and 7 kPa in the cylindrical channel. This difference in the limit is expected based on the d/λ criteria [1] because the orifice diameter (5.33 cm) is larger than the opening between fence obstacles in the square channel (3.81 cm). The continuity of the round tube data at 10 kPa shows that propagation in the round tube is not sensitive to whether a detonation wave or fast-flame leaves the square channel. For initial pressures between 12 and 25 kPa, the average velocity in both the square and round channels are very similar. However, for initial pressures greater than 25 kPa, the average velocity in the square channel is significantly higher than in the cylindrical channel. The difference in velocities may be attributed to the effects of curvature on detonation diffraction through the obstacle. For the square channel diffraction only occurs at the top and bottom of the channel when the wave propagates around the fence-type obstacle, essentially a 2D diffraction process. For the round tube diffraction occurs around the circumference of the orifice opening, essentially a three-dimensional diffraction process. The 3D diffraction in the orifice results in a faster decoupling of the detonation wave, resulting in a lower average velocity between plates. For fast-flames, higher average velocities were observed in the round tube. For fast flames since the energy released is not coupled to the lead shock, the severity of the diffraction is not important. As pointed out in [7] the interaction of the reflected shock with the flame governs the average flame velocity.

Based on the visualization results, propagation in the cylindrical channel can be characterized by four distinct modes: fast flame propagation (below 7 kPa), single hot spot ignition on the tube wall (7-15 kPa) and multi-head detonation (20-45 kPa), and a continuous detonation (50-60 kPa).

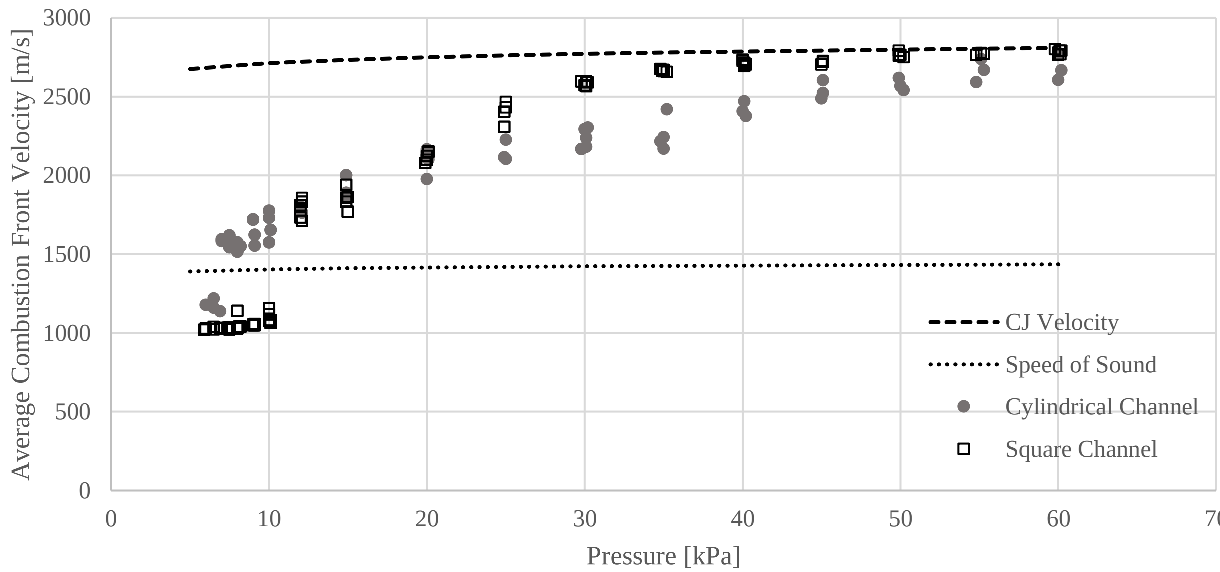

Figure 2: Average combustion front velocity in square and cylindrical channels as a function of initial pressure

A fast-flame, shown in Figure 3 for a test run at 6.5 kPa, consists of an uncoupled shock-flame complex. The flame is very faint, only becoming noticeable when the reflected shock originating from the orifice plate surface (not observable in Figure 3) traverses the flame. A distinguishing feature of the fast-flame is that shock reflection, off the tube wall or obstacle face, does not result in detonation initiation.

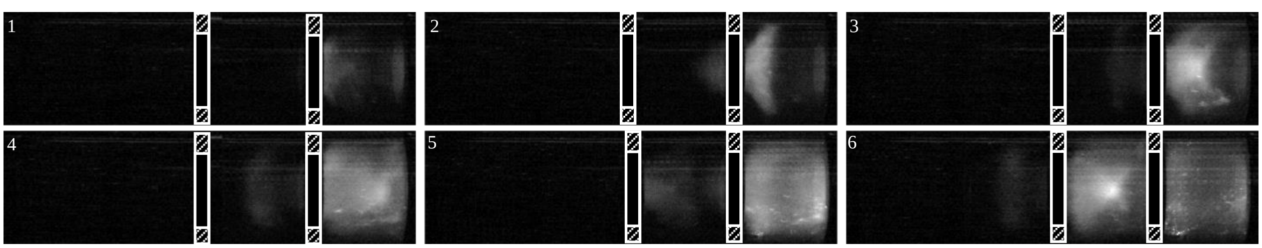

Figure 3: Test of stoichiometric oxygen-hydrogen mixture at 6.5 kPa filmed at 70,000 fps showing fast flame propagation between two orifice plates (Test 225)

For test pressures between 7 and 15 kPa, a single detonation kernel forms at the tube wall between orifice plates. Figure 4 shows the synchronized side and end-view video images from a test run at 10 kPa. The side-view spans consecutive orifice plates, including the downstream-edge of OP 8 (as marked by the vertical white line) and the upstream-face of OP 9 illuminated in image 6a. The end-view allows for the detonation front to be tracked as it interacts with the orifice plate face producing light that can be observed through the Acrylic orifice plates down the length of the tube. Note the detonation wave cannot be observed in the core of the orifice plates due to excessive light emitted by the combustion products over the length of the tube. A bright spot (with accompanying arrow showing the propagation direction) indicates a detonation initiation at the top wall of the tube in Image 2a, which grows radially in image 3a. The detonation wave collides with the top of the OP 9 first, as seen in image 4a, and spreads down and around the orifice plate, as indicated by the progression of the bright area seen in images 5a and 6a. This progression around the face of the orifice plate is seen in the end-view and is marked by arrows in images 4b, 5b and 6b. Due to the curvature of the tube wall the detonation wave is focused on the opposite side of the tube from where it was initiated, producing the bright light associated with the eroded plastic from the bottom of the OP 9 in image 6a. One would also expect that the transmitted wave through OP 9 would be biased in strength to the bottom part of the tube between OP 9 and 10 where the next ignition takes place. This pattern of alternating diametrically opposite ignition points continues down the length of the tube manifests itself as slapping waves propagating around the orifice plate face in the end-view video.

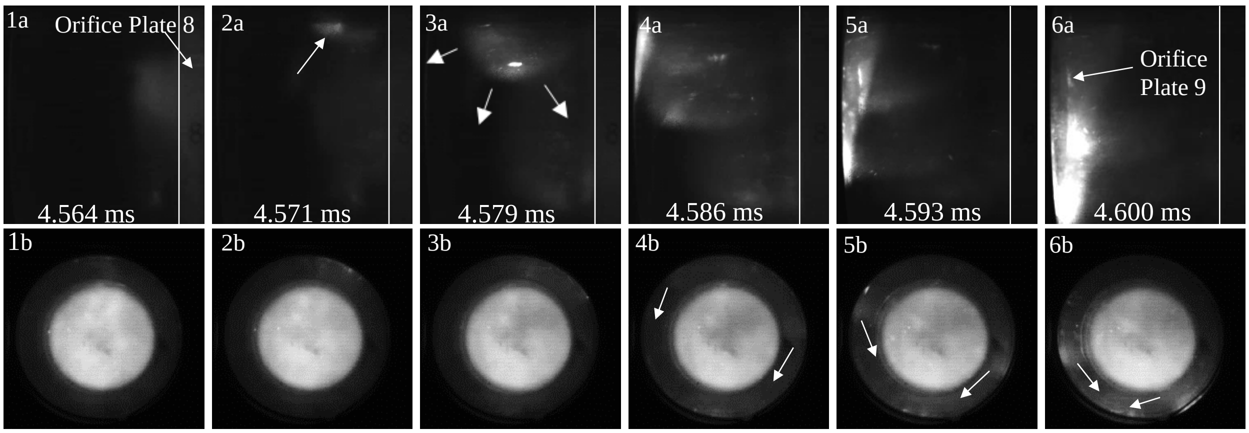

Figure 4: Test of stoichiometric hydrogen-oxygen mixture at 10 kPa (Test 86) filmed at 140,000 fps. Field-of-view between OP 8 and 9, wave propagation right to left. Top: Side-view; Bottom: End-view

A soot foil positioned after OP 9 from the test corresponding to the video in Figure 4, is provided in Figure 5. The single ignition site after OP 9 is circled on the foil and occurs after OP 9, roughly at the bottom of the tube. The two major triple-point trajectories are bordered by a band of very fine cell structure. The fine cell structure is caused by the overdriven detonation wave that propagates through the compressed unburned gas between the decoupled shock and flame.

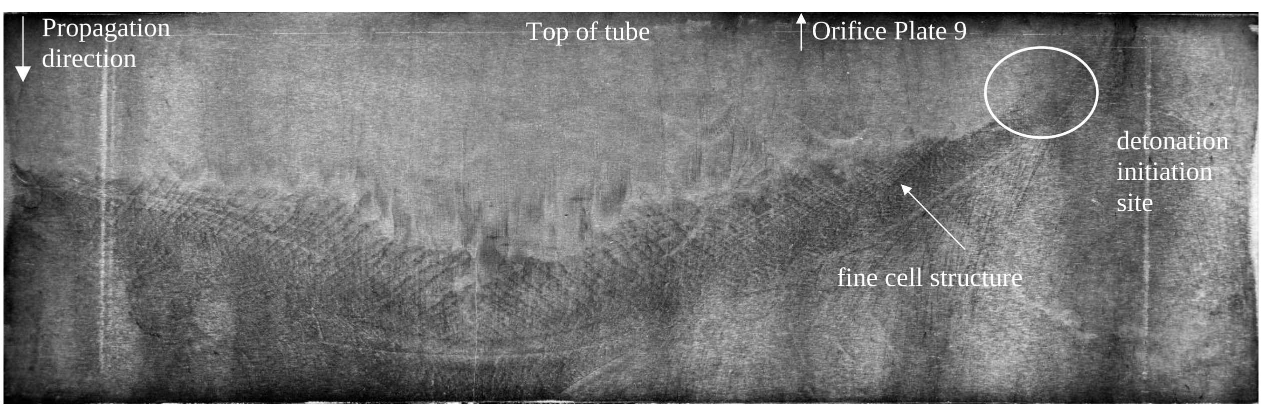

Figure 5: Soot foil obtained for 10 kPa stoichiometric hydrogen-oxygen mixture showing single point of detonation initiation (Test 86)

Higher initial pressures, between 20 and 45 kPa, yielded multiple detonation initiations along the wall of the cylinder. Figure 6 shows four side-view video images obtained for a 25 kPa test. In the first two images the detonation wave fails after passing through OP 8. After the decoupled shock (not observed in the image) reflects off the wall two hot spots form that develops into detonation waves (see arrows in image 3). The exact location of the detonation initiation on the wall is difficult to discern from the images, but it is clear that detonation initiation occurs before shock reflection off the upstream-face of OP 9, which is just to the left of the field-of-view.

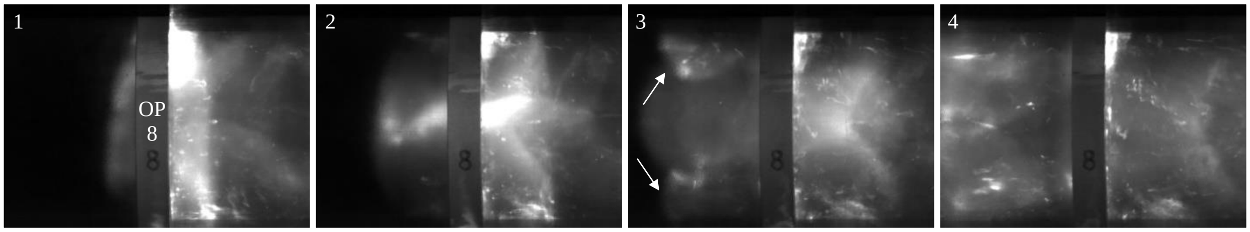

Figure 6: Video footage for stoichiometric hydrogen-oxygen mixture at 25 kPa (Test 75), camera speed 140,000 fps

A soot foil for higher pressure 40 kPa test in this regime (Figure 7) shows a cellular pattern typical of wall-reflection initiation of multiple detonation waves, arrows mark the point of ignition. This foil is similar to the foils obtained from tests performed in a steel tube with hydrogen-air mixtures at 1 bar, a detailed discussion of such foils can be found in [3]. The absence of cells immediately after OP 9 indicates that the detonation fails due to diffraction after the orifice plate (corroborated by Figure 7, image 2). In this test, there appears to be at least four spots that form into detonation waves.

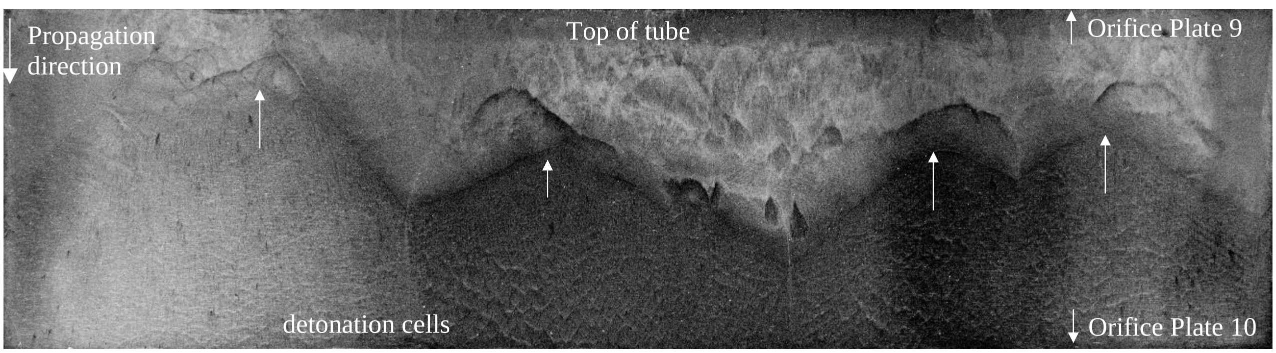

Figure 7: Soot foil for a 40 kPa stoichiometric hydrogen-oxygen mixture showing multiple points of detonation initiation (Test 158)

The continuous detonation regime (observed for initial pressures 50-60 kPa) is characterized by a detonation that does not fail along the centreline. End-view video footage was not completed for tests at pressures greater than 25 kPa. Due to the high reflected pressures generated, a dump tank was used instead of the optical end-plate. Figure 8 shows the side-view footage recorded for a 60 kPa test filmed at 70,000 fps.

For a similar 60 kPa test, a soot foil (Figure 9) installed vertically along the channel centreline between two orifice plates was used to verify that the detonation was continuous. Although the cells along the tube wall are slightly larger and more irregular due to diffraction, the cells along the centreline are a consistent size and pattern, indicating that the detonation did not fail due to diffraction there. Additional tests were filmed at 300,000 fps to track the combustion front along a narrow slit at the channel centreline. Consistent with a continuous detonation, the combustion front velocity was constant across the five-obstacle field-of-view.

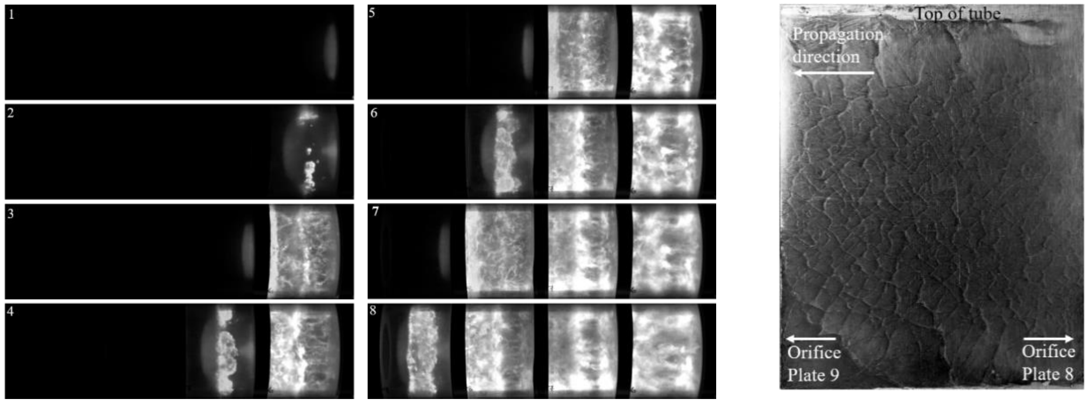

Figure 8: Left - Test of stoichiometric hydrogen-oxygen mixture at 60 kPa (Test 153) filmed at 70,000 fps. Right – Centreline soot foil for a similar 60 kPa stoichiometric hydrogen-oxygen test (Test 157)

4 Conclusions

High-speed photography was successfully used in conjunction with soot foils to visualize detonation propagation in an Acrylic round tube with equally spaced 50% blockage ratio orifice plates. The video results corroborate the interpretation of the detonation propagation mechanism proposed solely on soot foils in [3]. Single head-spin was not observed, instead near the limit a stable propagation mode was observed involving single hot spot wall ignition that alternated diametrically between orifice plates. The difference detonation propagation limits measured in the round and square tubes followed the traditional d/λ scaling. The higher detonation velocity deficit in the round tube was attributed to the more severe shock diffraction and detonation decoupling, compared to the 2D diffraction in the square channel. The severity of the diffraction did not affect the average fast-flame velocity since the shock and energy release are decoupled.

References

[1] Peraldi O, Knystautas R, Lee JH. (1988). Criteria for transition to detonation in tubes. Symp. (Int.) Combust. 21: 1629-1637.

[2] Lieberman D.H.B., Lee JHS (2001). Photographic study of the transition between the quasi-detonation and choking regimes. 18th International Colloquium on the Dynamics of Explosion and Reactive Systems.

[3] Ciccarelli G, Cross M (2016). On the propagation mechanism of a detonation wave in a round tube with orifice plates. Shock Waves 26(5):587-597.

[4] Starr A, Lee JH, Ng HD (2015) Detonation limits in rough walled tubes. Proc. Combust. Inst. 35(2): 1989-1996.

[5] Teodorcyzk A, Lee JH, Knystautas R. (1988) Propagation mechanism of quasi-detonations. Proc. Combust. Inst. 22: 1723-1731.

[6] Kellenberger M, Ciccarelli G (2015) Investigation of quasi-detonation propagation using simultaneous soot foil and schlieren photography. International Colloquium on the Dynamics of Explosion and Reactive Systems, Leeds.

[7] Kellenberger M, Ciccarelli G (2015) Propagation Mechanism of Supersonic Combustion Waves. Proc. Combust. Inst. 35 (2015) 2109–2116.